

# Low-Temperature Conversion of Methane to Methanol on CeO<sub>x</sub>/Cu<sub>2</sub>O Catalysts: Water Controlled Activation of the C–H Bond

Zhijun Zuo,<sup>†</sup> Pedro J. Ramírez,<sup>‡</sup> Sanjaya D. Senanayake,<sup>§</sup> Ping Liu,<sup>\*,§</sup> and José A. Rodríguez<sup>\*,§</sup>

<sup>†</sup>Key Laboratory of Coal Science and Technology of Ministry of Education and Shanxi Province, Taiyuan University of Technology, Taiyuan 030024, Shanxi, China

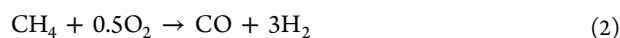
<sup>‡</sup>Facultad de Ciencias, Universidad Central de Venezuela, Caracas 1020-A, Venezuela

<sup>§</sup>Chemistry Department, Brookhaven National Laboratory, Upton, New York 11973, United States

**S** Supporting Information

**ABSTRACT:** An inverse CeO<sub>2</sub>/Cu<sub>2</sub>O/Cu(111) catalyst is able to activate methane at room temperature producing C, CH<sub>x</sub> fragments and CO<sub>x</sub> species on the oxide surface. The addition of water to the system leads to a drastic change in the selectivity of methane activation yielding only adsorbed CH<sub>x</sub> fragments. At a temperature of 450 K, in the presence of water, a CH<sub>4</sub> → CH<sub>3</sub>OH catalytic transformation occurs with a high selectivity. OH groups formed by the dissociation of water saturate the catalyst surface, removing sites that could decompose CH<sub>x</sub> fragments, and generating centers on which methane can directly interact to yield methanol.

Methane is the main component of natural gas. The high abundance of methane in our planet makes it an attractive fuel and building block for the production of fine commodity chemicals.<sup>1</sup> Development of a method for a direct conversion of methane to methanol can lead to a major commercial breakthrough in the use of methane.<sup>1</sup> The partial oxidation of methane to methanol is challenging because the reaction typically progresses all the way to yield CO and/or CO<sub>2</sub>.<sup>2</sup>



Reactions 1 and 2 are both exothermic, and at temperatures above 600 K reaction 2 becomes the preferred pathway from a thermodynamic viewpoint.<sup>2</sup> Thus, to trap the methanol as a product or intermediate, it is essential to find materials that can activate methane in an efficient way at low temperatures (<500 K).<sup>2,3</sup> This is difficult because the C–H bond in CH<sub>4</sub> has the highest bond energy (104 kcal/mol) among organic compounds. The growing need for inexpensive methods to convert methane to methanol has sparked considerable interest in different approaches that catalyze this process.<sup>3–9</sup> The enzyme methane monooxygenase produces methanol from methane, but cannot be used for industrial-scale reactions.<sup>4,7</sup> In the enzyme, the conversion process is probably carried out by a group of three copper ions.<sup>4</sup> It has been found that copper-exchange zeolites can mimic the nuclearity and reactivity of active sites of the methane monooxygenase.<sup>3,9</sup> In the structure of the zeolites, methanol can be produced by sequential dosing

of O<sub>2</sub> and methane, and then flushed out with water.<sup>3</sup> A direct catalytic transformation of methane to methanol is also possible.<sup>9</sup> In this study, we show that a CeO<sub>2</sub>/Cu<sub>2</sub>O/Cu(111) inverse system is able to activate methane at room temperature and then, with the help of water, performs a catalytic cycle, which is highly selective to the production of methanol.

The system under investigation in this study consists of a film of Cu<sub>2</sub>O partially covered with ceria nanoparticles.<sup>10–13</sup> Its morphology has been studied in detail with scanning tunneling microscopy (STM) and low-energy electron microscopy (LEEM).<sup>10,12,13</sup> On the Cu<sub>2</sub>O substrate, ceria grows forming small islands (2–5 nm in size) that appear on the terraces of the surface, and large islands (30–50 nm in size) which are embedded in the substrate step edges.<sup>10,13</sup> The large ceria islands have a morphology different from that for the two most stable surfaces of bulk ceria: CeO<sub>2</sub>(111) and CeO<sub>2</sub>(110).<sup>10,13</sup> At small and medium coverages of ceria (<0.5 ML), the islands are essentially a single layer of ceria {O–Ce–O–Cu staking}.<sup>10,13</sup> At larger coverages, the appearance of islands with two or three ceria layers is observed.<sup>10,13</sup> The oxygen content of the ceria islands easily changes after exposing them to reducing agents or after reoxidation with O<sub>2</sub> or water.<sup>10,13</sup> From previous studies, it is known that the CeO<sub>2</sub>/Cu<sub>2</sub>O/Cu(111) system is quite active for the dissociation of O<sub>2</sub> and H<sub>2</sub>O and is an excellent catalyst for the oxidation of CO (O<sub>2</sub> + 2CO → 2CO<sub>2</sub>) and the PROX process.<sup>10,14</sup>

We investigated the dissociation of methane on a series of CeO<sub>2</sub>/Cu<sub>2</sub>O/Cu(111) surfaces at room temperature. Figure 1 shows C 1s XPS spectra collected after exposing a plain Cu<sub>2</sub>O film and a film covered ~40% with ceria to 1 Torr of CH<sub>4</sub> at 300 K for 5 min. On the plain Cu<sub>2</sub>O film, the adsorption of methane is negligible. In contrast, the CeO<sub>2</sub>/Cu<sub>2</sub>O surface activates methane. Clear peaks are shown in Figure 1 for carbon, CH<sub>x</sub> and CO<sub>x</sub> species.<sup>15,16</sup> A fraction of the adsorbed methane undergoes complete decomposition: CH<sub>4</sub> → CH<sub>3</sub> → CH<sub>2</sub> → CH → C. Some of the generated C adatoms react with O atoms from the surface to form CO<sub>x</sub> species. Less than a monolayer of methane react with the CeO<sub>2</sub>/Cu<sub>2</sub>O/Cu(111) surface and the changes in the oxidation state of Cu and Ce were negligible. The ability of CeO<sub>2</sub>/Cu<sub>2</sub>O/Cu(111) to dissociate water,<sup>13</sup> H<sub>2</sub>O → OH + H, can be used to control

Received: August 18, 2016

Published: October 10, 2016

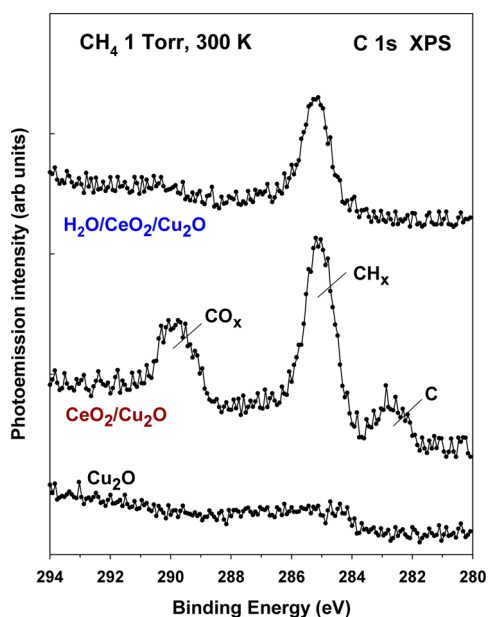


**Figure 1.** C 1s XPS spectra collected after exposing  $\text{Cu}_2\text{O}/\text{Cu}(111)$ ,  $\text{CeO}_2/\text{Cu}_2\text{O}/\text{Cu}(111)$  and  $\text{H}_2\text{O}/\text{CeO}_2/\text{Cu}_2\text{O}/\text{Cu}(111)$  to 1 Torr of methane at 300 K for 5 min. In the  $\text{CeO}_2/\text{Cu}_2\text{O}/\text{Cu}(111)$  system,  $\sim 40\%$  of the  $\text{Cu}_2\text{O}$  film was covered by ceria. To generate the  $\text{H}_2\text{O}/\text{CeO}_2/\text{Cu}_2\text{O}/\text{Cu}(111)$  sample, the  $\text{CeO}_2/\text{Cu}_2\text{O}/\text{Cu}(111)$  surface was exposed to 50 Langmuir of water at 300 K.

the activation of methane. If water is preadsorbed to  $\text{CeO}_2/\text{Cu}_2\text{O}$ , the selectivity toward the production of  $\text{CH}_x$  increases to 100% (top spectrum in Figure 1). Surface sites that are highly active for the full decomposition of methane are probably blocked by OH groups and the signals for C and  $\text{CO}_x$  species disappear from the C 1s region. As shown below, this phenomenon can greatly facilitate the conversion of methane into methanol.

The deposited  $\text{CH}_x$  species in the surfaces of Figure 1 desorbed when the sample temperature was increased from 300 to 400 K. These species are not observed when the  $\text{CeO}_2/\text{Cu}_2\text{O}/\text{Cu}(111)$  is exposed to methane at 450 K (see Figure S1 in Supporting Information). At this temperature, if water is not present in the background, a large amount of carbon is deposited on the surface (Figure S1) and there is a substantial reduction of the  $\text{CeO}_2$  and  $\text{Cu}_2\text{O}$  present in the sample. At 450 K, the mixed-metal oxide is extremely efficient for the cleavage of all the C–H bonds of methane and the generated C and H atoms react with O sites from  $\text{Cu}_2\text{O}$  and  $\text{CeO}_2$  to produce CO and  $\text{H}_2\text{O}$ . When the C-rich surface obtained by exposing  $\text{CeO}_2/\text{Cu}_2\text{O}$  to methane at 450 K was treated with water, there was a very large reduction in the intensity of the C features in the C 1s region (Figure S2).

We found that the  $\text{CH}_x$  and OH groups coadsorbed on  $\text{CeO}_2/\text{Cu}_2\text{O}/\text{Cu}(111)$  did not react to yield methanol at room temperature. The system cannot overcome the activation barriers associated with the cleavage of HO–surface and  $\text{H}_x\text{C}$ –surface bonds. No reaction was also observed after dosing  $\text{CH}_4$  to  $\text{OH}/\text{CeO}_2/\text{Cu}_2\text{O}$  or  $\text{H}_2\text{O}$  to  $\text{CH}_x/\text{CeO}_2/\text{Cu}_2\text{O}$  at 300 K. However, at 450 K, we detected formation of methanol. Figure 2 shows data for the conversion of methane into methanol at 450 K under a water-rich environment. Plain  $\text{Cu}_2\text{O}$  is inert as a catalyst. As ceria is added to the copper oxide, there is an increase in the catalytic production of methanol and  $\text{CO}/\text{CO}_2$  are only secondary products. At the maximum of catalytic activity the ratio of methanol to  $\text{CO}/\text{CO}_2$  is close to 3:1. The

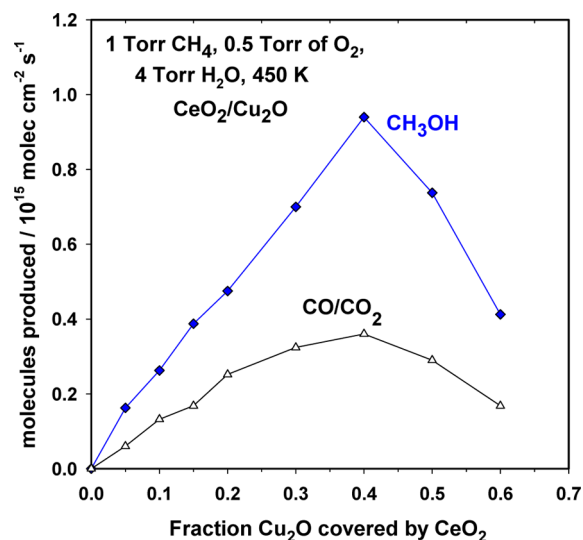


**Figure 2.** Production of methanol and  $\text{CO}/\text{CO}_2$  as a function of ceria coverage in a series of  $\text{CeO}_2/\text{Cu}_2\text{O}/\text{Cu}(111)$  catalysts. The samples were exposed to 1 Torr of  $\text{CH}_4$ , 0.5 Torr of  $\text{O}_2$  and 4 Torr of  $\text{H}_2\text{O}$  at 450 K in a batch reactor.

drop in catalytic activity shown in Figure 2 for large ceria coverages matches well with changes in STM for the growth mode of ceria on  $\text{Cu}_2\text{O}/\text{Cu}(111)$ .<sup>10,13</sup> When less than 50% of the copper oxide is covered, the ceria islands have only a single layer (i.e., O–Ce–O–Cu staking), but two- and three-layer islands are observed at higher ceria coverages.<sup>10,13</sup> Thus, active sites are probably present at the interface of single-layer ceria islands and  $\text{Cu}_2\text{O}$ .

The pressure of water had a strong effect on the selectivity toward the production of methanol. In Figure 3, we compare

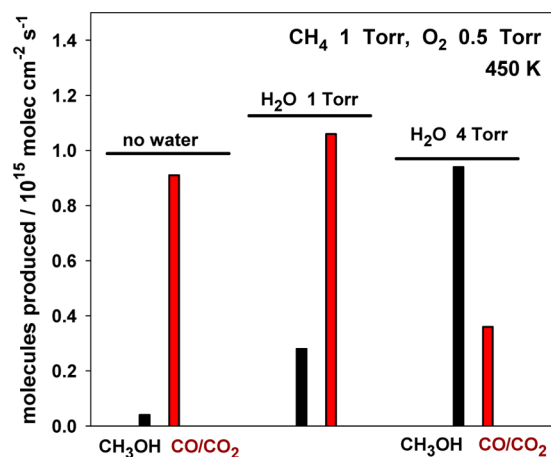


**Figure 3.** Production of methanol and  $\text{CO}/\text{CO}_2$  as a function of water pressure on a  $\text{CeO}_2/\text{Cu}_2\text{O}/\text{Cu}(111)$  catalyst in which  $\sim 40\%$  of the  $\text{Cu}_2\text{O}$  was covered by ceria. The samples were exposed to 1 Torr of  $\text{CH}_4$ , 0.5 Torr of  $\text{O}_2$  and 0, 1, or 4 Torr of  $\text{H}_2\text{O}$  at 450 K in a batch reactor.

the amounts of methanol and  $\text{CO}/\text{CO}_2$  formed as a function of the water pressure in the reactant mixture. If water is not present, the amount of methanol formed is minimal. The highly active sites of the surface are not blocked and the reaction  $\text{CH}_4 + n\text{O}_2 \rightarrow \text{CO}/\text{CO}_2$  takes place instead of methanol formation. In fact, both reactions are feasible from a thermodynamic viewpoint,<sup>2</sup> but most of the methanol formed may be

decomposed into CO/CO<sub>2</sub>.<sup>3</sup> As water is added, the selectivity toward methanol clearly improves in Figure 3. In a set of experiments, we found that preadsorbing with water blocks the surface sites which are active in CeO<sub>2</sub>/Cu<sub>2</sub>O/Cu(111) for the dissociation of the methanol molecule. These sites are probably the same sites that carry out the full decomposition of methane in clean CeO<sub>2</sub>/Cu<sub>2</sub>O/Cu(111). In principle, water could be helping the CH<sub>4</sub> → CH<sub>3</sub>OH conversion in two ways: Blocking active sites for the dissociation of methanol or by opening a new reaction path for the direct reaction of CH<sub>4</sub> or CH<sub>3</sub> with OH groups. These two possibilities were explored using calculations based on density-functional theory (DFT) (see SI for details).

Postreaction characterization of the catalysts used for the experiments in Figure 3 with XPS showed that their surfaces contained Ce<sup>4+</sup> and Cu<sup>1+</sup> (i.e., no reduction of the components in the CeO<sub>2</sub>/Cu<sub>2</sub>O/Cu(111) starting catalysts). The interaction of methane with Cu<sub>2</sub>O/Cu(111) and CeO<sub>2</sub>/Cu<sub>2</sub>O/Cu(111) surfaces was investigated employing models developed in previous studies.<sup>10,17</sup> Top and side views of these models are shown in Figure S3. From the results in Figure 2 and previous STM studies,<sup>10,13</sup> we know that the active phase of the catalyst contains single-layer ceria islands dispersed on Cu<sub>2</sub>O. The calculated adsorption energies of reaction intermediates on Cu<sub>2</sub>O/Cu(111) and CeO<sub>2</sub>/Cu<sub>2</sub>O/Cu(111) are listed in Table S1. One can see that the deposition of CeO<sub>2</sub> leads to a stabilization of the CH<sub>3</sub> and OH intermediates. The calculations indicate that on both surfaces, methane is only physisorbed. The dissociation of methane on a Cu<sub>2</sub>O/Cu(111) surface is problematic (reaction energy of 0.30 eV and activation barrier of 1.60 eV) in agreement with the XPS data in Figure 1. With the presence of CeO<sub>2</sub> nanoparticles on the Cu<sub>2</sub>O film, the interfacial Ce<sup>4+</sup> sites help methane dissociation to methyl (reaction energy of −1.23 eV and activation energy of 0.51 eV) at the interfacial O sites (Figure 4). Thus, methane

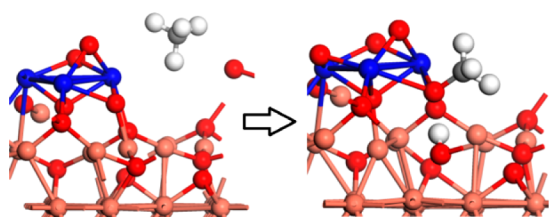


**Figure 4.** Calculated adsorption geometry for methane adsorption and dissociation on CeO<sub>2</sub>/Cu<sub>2</sub>O/Cu(111). The blue, brown, red, gray and white balls represent Ce, Cu, O, C and H atoms, respectively.

can dissociate on CeO<sub>2</sub>/Cu<sub>2</sub>O/Cu(111) at room temperature. The calculated activation energy is much smaller than typical values found on metals,<sup>8,18</sup> A key factor is the participation of the O centers of CeO<sub>2</sub>/Cu<sub>2</sub>O/Cu(111) in C–H bond breaking (Figure 4). The calculated activation energy of 0.51 eV compares well with activation energies found for systems that can activate methane at room temperature like Zn modified H-ZSM-5<sup>6</sup> and Ni dispersed on ceria.<sup>15</sup>

The deposition of CeO<sub>2</sub> also helps water dissociation. On Cu<sub>2</sub>O/Cu(111), water dissociation is an activated process (reaction energy of 0.33 eV and activation energy of 0.84 eV). The presence of CeO<sub>2</sub> enables a spontaneous O–H bond cleavage. Although the dissociation of methane on CeO<sub>2</sub>/Cu<sub>2</sub>O is energetically favorable; yet it cannot compete with water dissociation at the same sites. Therefore, surface hydroxylation

is expected, and water should have strong effect in the selectivity of the reaction processes. The calculations indicate that following the Langmuir–Hinshelwood (LH) mechanism the reaction involving dissociated CH<sub>3</sub>(ads) at the interfacial O sites and OH(ads) at Ce sites to yield methanol is rather difficult (reaction energy of 0.48 eV and activation barrier of 2.80 eV, Figure S4). This is likely hindered by the high stability of CH<sub>3</sub>(ads) at the oxygen sites. The reaction could follow less direct paths in which methyl reacts with O to form CH<sub>3</sub>O and then is hydrogenated to form methanol, as proposed in other theoretical studies.<sup>6,9</sup> One interesting route found in the DFT calculations involves a direct dissociation of methane on the dissociated OH groups bound to Cu<sub>2</sub>O or CeO<sub>2</sub>/Cu<sub>2</sub>O via the Eley–Rideal (ER) mechanism, see Figures 5 and S5 plus Table

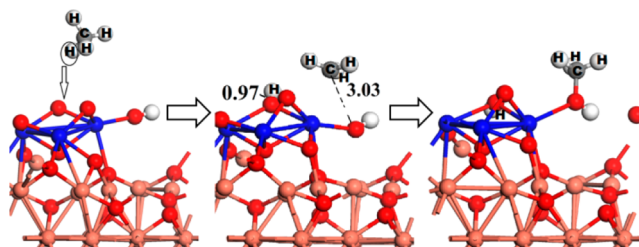


**Figure 5.** Structures of initial (left), transition (middle) and final (right) states for methanol synthesis involving dissociative adsorption of methane over the OH(ads) species on CeO<sub>2</sub>/Cu<sub>2</sub>O/Cu(111). The blue, brown, red, gray and white balls represent Ce, Cu, O, C and H atoms, respectively.

S2. Following this pathway on HO/CeO<sub>2</sub>/Cu<sub>2</sub>O/Cu(111), the dissociation of methane leads to the direct formation of methanol at the OH anchored at Ce sites and avoids the cleavage of strong O–CH<sub>3</sub> bonds. As a result, the methanol formation is greatly facilitated (reaction energy of −0.75 eV and activation energy of 1.22 eV, Figure S5). The calculations show that without the use of the OH bound to Ce sites, the methyl species from methane dissociation at interfacial Ce sites are too stable to be oxidized, rather preferring further decomposition to carbon. However, this is not the case for Cu<sub>2</sub>O/Cu(111). Although the surface hydroxylation is also likely to occur, the direct methane dissociation on OH(ads) is highly activated with the barriers of at least 1.93 eV depending on the position of OH(ads) (Figures S6 and S7). On Cu<sub>2</sub>O/Cu(111), the OH is embedded on a hexagonal cavity of the oxide surface (Figure S6); a configuration that makes difficult interactions with methane (Figure S7). This is not a problem in the case of OH bound to CeO<sub>2</sub>/Cu<sub>2</sub>O/Cu(111), Figure 5. The high activity of the OH(ads) species bound to CeO<sub>2</sub>/Cu<sub>2</sub>O/Cu(111) is also associated with a hybridization between O 2p orbitals and 4f orbitals of Ce<sup>4+</sup>. It results in an OH species with intense high-lying O 2p states, which are more active for attracting and dissociating methane than OH(ads) bound to Cu<sub>2</sub>O/Cu(111), see Figure 6.

In summary, we have found that a CeO<sub>2</sub>/Cu<sub>2</sub>O interface is able to bind and dissociate methane at room temperature. In this aspect, it mimics the activity of the methane monooxygenase<sup>4</sup> and a few inorganic systems.<sup>5,6,19</sup> The products of the adsorption process on CeO<sub>2</sub>/Cu<sub>2</sub>O are C, CH<sub>x</sub> fragments and CO<sub>x</sub> species. The addition of water to the system leads to a drastic change in the selectivity of methane activation yielding only adsorbed CH<sub>x</sub> fragments. At a temperature of 450 K, in the presence of water, a CH<sub>4</sub> → CH<sub>3</sub>OH catalytic trans-

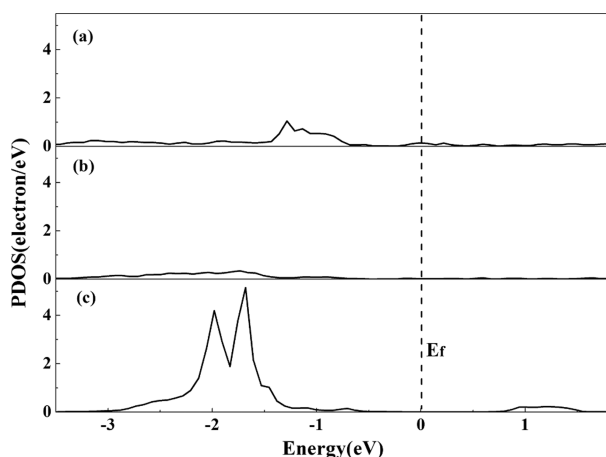


**Figure 6.** O 2p PDOS for OH(ads) in the ring center (a) and at atop (b) sites of Cu ions on Cu<sub>2</sub>O/Cu(111), and top of Ce ions on CeO<sub>2</sub>/Cu<sub>2</sub>O/Cu(111) (c). States with high intensity are observed only in the case of OH/CeO<sub>2</sub>/Cu<sub>2</sub>O/Cu(111).

formation occurs with a high selectivity. OH groups formed by the dissociation of water saturate the catalyst surface, removing sites that could decompose CH<sub>x</sub> fragments, and generating centers, which have special electronic properties, on which methane can directly interact to yield methanol.

## ■ ASSOCIATED CONTENT

### 📄 Supporting Information

The Supporting Information is available free of charge on the ACS Publications website at DOI: 10.1021/jacs.6b08668.

Experimental procedures; C 1s XPS spectra collected after dosing methane and water to a CeO<sub>2</sub>/Cu<sub>2</sub>O system at 450 K; details for the DFT calculations; structures of the models used in DFT calculations to describe bare Cu<sub>2</sub>O/Cu(111) and CeO<sub>2</sub>/Cu<sub>2</sub>O/Cu(111) surfaces systems as well as some of the reaction intermediates and transition states involved (PDF)

## ■ AUTHOR INFORMATION

### Corresponding Authors

\*P.L. [pingliu3@bnl.gov](mailto:pingliu3@bnl.gov)

\*J.A.R. [rodriguez@bnl.gov](mailto:rodriguez@bnl.gov)

### Notes

The authors declare no competing financial interest.

## ■ ACKNOWLEDGMENTS

The research carried out at Brookhaven National Laboratory was supported by the U.S. Department of Energy, Office of Science and Office of Basic Energy Sciences under Contract No. DE-SC0012704. The DFT calculations were performed using computational resources at the Center for Functional Nanomaterials, a user facility at Brookhaven National Laboratory. P.J.R. (UCV) is grateful for partial support of INTEVEP and the BID. Z.Z. also gratefully acknowledges the National High Technology Research and Development Program of China (2013AA051201), the key project of the National Natural Science Foundation of China (21336006), and the National Natural Science Foundation of China (21306125) for financial support.

## ■ REFERENCES

- (1) *Methane in the Environment: Occurrence, Uses and Pollution*, Basile, A., Ed.; Nova Science Publications Inc.: New York, 2013.
- (2) Khirsariya, P.; Mewada, R. K. *Procedia Eng.* **2013**, *51*, 409–415.
- (3) (a) Grundner, S.; Markovits, M. A. C.; Li, G.; Tromp, M.; Pidko, E. A.; Hensen, E. J. M.; Jentys, A.; Sanchez-Sanchez, M.; Lercher, J. A. *Nat. Commun.* **2015**, *6*, 7546–7555. (b) Li, G.; Vassilev, P.; Sanchez-Sanchez, M.; Lercher, J. A.; Hensen, E. J. M.; Pidko, E. A. *J. Catal.* **2016**, *338*, 305–312.
- (4) Chan, S. I.; Yu, S.S.-F. *Acc. Chem. Res.* **2008**, *41*, 969–979.
- (5) Chan, S. I.; Lu, Y. J.; Nagababu, P.; Maji, S.; Hung, M. C.; Lee, M. M.; Hsu, I. J.; Minh, P. D. M.; Lai, J. C. H.; Ng, K. Y.; Ramalingam, S.; Yu, S. F.; Chan, M. K. *Angew. Chem., Int. Ed.* **2013**, *52*, 3731–3735.
- (6) Xu, J.; Zheng, A.; Wang, X.; Qi, G.; Su, J.; Du, J.; Gan, Z.; Wu, J.; Wang, W.; Deng, F. *Chem. Sci.* **2012**, *3*, 2932–2940.
- (7) Olivos-Suarez, A. I.; Szécsényi, A.; Hensen, E. J. M.; Ruiz-Martinez, J.; Pidko, E. A.; Gascon, J. *ACS Catal.* **2016**, *6*, 2965–2981.
- (8) Chin, Y.-H.; Buda, C.; Neurock, M.; Iglesia, E. *J. Am. Chem. Soc.* **2013**, *135*, 15425–15442.
- (9) (a) Narsimhan, K.; Iyoki, K.; Dinh, K.; Román-Leshkov, Y. *ACS Cent. Sci.* **2016**, *2*, 424–429. (b) Tomkins, P.; Mansouri, A.; Bozbag, S. E.; Krumeich, F.; Park, M. B.; Alayon, E. M. C.; Ranocchiari, M.; van Bokhoven, J. A. *Angew. Chem., Int. Ed.* **2016**, *55*, 5467–5471.
- (10) Yang, F.; Graciani, J.; Evans, J.; Liu, P.; Hrbek, J.; Sanz, J. F.; Rodriguez, J. A. *J. Am. Chem. Soc.* **2011**, *133*, 3444–3451.
- (11) Senanayake, S.; Sadowski, J. T.; Evans, J.; Kundu, S.; Agnoli, S.; Yang, F.; Stacchiola, D.; Flege, J. I.; Hrbek, J.; Rodriguez, J. A. *J. Phys. Chem. Lett.* **2012**, *3*, 839–843.
- (12) Yang, F.; Choi, Y. M.; Agnoli, S.; Liu, P.; Stacchiola, D.; Hrbek, J.; Rodriguez, J. A. *J. Phys. Chem. C* **2011**, *115*, 23062–23066.
- (13) Rodriguez, J. A.; Graciani, J.; Evans, J.; Park, J. B.; Yang, F.; Stacchiola, D.; Senanayake, S. D.; Ma, S.; Perez, M.; Liu, P.; Sanz, J. F.; Hrbek, J. *Angew. Chem., Int. Ed.* **2009**, *48*, 8047–8050.
- (14) Hornés, A.; Hungria, A. B.; Bera, P.; López Cámara, A.; Fernández-García, M.; Martínez-Arias, A.; Barrio, L.; Estrella, M.; Zhou, G.; Fonseca, J. J.; Hanson, J. C.; Rodriguez, J. A. *J. Am. Chem. Soc.* **2010**, *132*, 34–35.
- (15) Liu, Z.; Grinter, D. C.; Lustemberg, P. G.; Nguyen-Phan, T. D.; Zhou, Y.; Luo, S.; Waluyo, I.; Crumlin, E. J.; Stacchiola, D. J.; Zhou, J.; Carrasco, J.; Busnengo, F.; Ganduglia-Pirovano, V.; Senanayake, S. D.; Rodriguez, J. A. *Angew. Chem., Int. Ed.* **2016**, *55*, 7455–7459.
- (16) Liu, Z.; Duchoň, T.; Wang, H.; Peterson, E. W.; Zhou, Y.; Luo, S.; Zhou, J.; Matolín, V.; Stacchiola, D. J.; Rodriguez, J. A.; Senanayake, S. D. *J. Phys. Chem. C* **2015**, *119*, 18248–18256.
- (17) (a) An, W.; Xu, F.; Stacchiola, D.; Liu, P. *ChemCatChem* **2015**, *7*, 3865–3872. (b) An, W.; Baber, A. E.; Xu, F.; Soldemo, M.; Weissenrieder, J.; Stacchiola, D.; Liu, P. *ChemCatChem* **2014**, *6*, 2364–2372.
- (18) Choudhary, T. V.; Aksoylu, E.; Goodman, D. W. *Catal. Rev.: Sci. Eng.* **2003**, *45*, 151–203.
- (19) Hammond, C.; Dimitratos, N.; Lopez-Sanchez, J. A.; Jenkins, R. L.; Whiting, G.; Kondrat, S. A.; ab Rahim, M. H.; Forde, M. M.; Thetford, A.; Hagen, H.; Stangland, E. E.; Moulijn, J. M.; Taylor, S. H.; Willock, D. J.; Hutchings, G. J. *ACS Catal.* **2013**, *3*, 1835–1844.